The Journal of Veterinary Medical Science

NOTE

Internal Medicine

Change in right ventricular function in an American cocker spaniel with acute pulmonary thromboembolism

Tomoya MORITA[1)], Kensuke NAKAMURA[2)]*, Tatsuyuki OSUGA[3)], Kiwamu HANAZONO[3)], Keitaro MORISHITA[3)] and Mitsuyoshi TAKIGUCHI[1)]

[1)]Laboratory of Veterinary Internal Medicine, Department of Veterinary Clinical Sciences, Graduate School of Veterinary Medicine, Hokkaido University, N18 W9, Sapporo, Hokkaido 060-0818, Japan
[2)]Organization for Promotion of Tenure Track, University of Miyazaki, 1-1 Gakuenkibanadai-nishi, Miyazaki 889-2192, Japan
[3)]Veterinary Teaching Hospital, Department of Veterinary Clinical Sciences, Graduate School of Veterinary Medicine, Hokkaido University, N18 W9, Sapporo, Hokkaido 060-0818, Japan

J. Vet. Med. Sci.
81(9): 1259–1265, 2019
doi: 10.1292/jvms.19-0082

Received: 7 February 2019
Accepted: 27 June 2019
Advanced Epub: 9 July 2019

ABSTRACT. A 12-year-old neutered female American cocker spaniel weighing 9.9 kg was presented for evaluation with a 2-day history of dyspnea and anorexia. Echocardiography revealed severe pulmonary hypertension (estimated systolic pulmonary arterial pressure, 93.4 mmHg) with right heart enlargement, pulmonary arterial dilation, and right ventricular dysfunction. The dilation of left heart and congenital cardiac shunt were not observed. Pulmonary thromboembolism (PTE) was confirmed by computed tomographic angiography. After treatment with antiplatelet and anticoagulant, the clinical sign and the echocardiographic abnormality of right heart were improved. These echocardiographic findings are not specific for PTE, but it can be useful as a rule-in test for PTE when other causes of pulmonary hypertension are excluded and a monitor of therapeutic efficacy.

KEY WORDS: acute pulmonary thromboembolism, dog, echocardiography, myocardial hypokinesis

Acute pulmonary thromboembolism (PTE) is a life-threatening disease characterized by the obstruction of a pulmonary artery or arteries by a thrombus, leading to right ventricular (RV) pressure overload, RV dysfunction, hypotension, cardiogenic shock, and ultimately death [9]. In human patients with acute PTE, the 30-day all-cause mortality rate is between 9 and 11%, and 3-month mortality rates are between 8.6 and 17% [9]. The prevalence rate of PTE in dogs was reported to be 0.9% over a 10-year period [7]. In human medicine, definitive diagnosis of PTE is made by computed tomography (CT) angiography. However, in veterinary medicine, CT angiography is not routinely used. While echocardiography may be useful for assessment in dogs with suspected PTE due to its non-invasiveness, there are few data on echocardiographic findings in dogs with PTE. In this case report, the author describes the changes in echocardiographic indices in a case of the severe pulmonary hypertension (PH) due to acute PTE diagnosed by CT angiography.

A 12-year-old neutered female American cocker spaniel weighing 9.9 kg (BCS 3/5) was presented for evaluation with a 2-day history of dyspnea and anorexia. The dog had been diagnosed 8 days prior with gallbladder mucocele, pancreatitis, and extrahepatic bile duct obstruction. Two days later, the gallbladder mucocele was surgically removed, and the dog was discharged 4 days after surgery.

On presentation, the dog was lethargic and physical examination revealed tachypnea and respiratory distress. The heart rate was 128 bpm, and heart murmur was not auscultated. The SpO_2 was not measurable by pulse oximetry. Systolic and diastolic blood pressure measurement with an oscillometric blood pressure measurement instrument (PetMAP Graphic, Ramsey Medical Inc., Tampa, FL, U.S.A.) did not confirm systemic hypotension (systolic, 162 mmHg [reference interval, 140–150 mmHg]; diastolic, 69 mmHg [reference interval, 83.0–91.6 mmHg]) [1].

Complete blood cell count was carried out using automated hemocytometer (MEK-6500 Celltac α, Nihon Kohden Co., Tokyo, Japan). Significant findings from the complete blood count were leukocytosis ($38.3 \times 10^3/\mu l$ [reference range, $5.1–16.8 \times 10^3/\mu l$]) and thrombocytopenia ($103 \times 10^3/\mu l$ [reference range, $148–488 \times 10^3/\mu l$]). The serum biochemical profile was carried out using biochemical analyzer (Fuji DRI-CHEM 7000, FUJIFILM Medical Co., Ltd., Tokyo, Japan). The serum biochemical profile was within the normal range. Prothrombin time, activated partial thromboplastin time, and fibrinogen were carried out using

*Correspondence to: kenvet@cc.miyazaki-u.ac.jp

automated blood coagulation analyzer (COAG2V, FUJIFILM Wako Pure Chemical Corp., Osaka, Japan). Prothrombin time was 8.0 sec [reference interval, 7.4–8.8 sec], activated partial thromboplastin time was 21.1 sec [reference interval, 12.0–28.0 sec], and fibrinogen was 344 mg/d*l* [150–350 mg/d*l*].

The thoracic radiographs revealed cardiac enlargement (VHS, 11.75), enlargement of the main pulmonary artery (PA) in left and right caudal lobes, and interstitial and alveolar lung patterns in the right cranial, middle, and left cranial lobes (Fig. 1A and 1B).

Transthoracic echocardiography performed with an ultrasound unit (Artida, Canon Medical Systems Corp., Tochigi, Japan) equipped with a 3–6 MHz sector probe (PST-50BT, Canon Medical Systems Corp.). Echocardiographic variables are summarized in Table 1. Transthoracic echocardiography demonstrated severe RV, right atrial (RA), and main PA dilation (PA to aorta ratio, 1.24 [reference range, <0.98 [14]]). The RV to left ventricular end-diastolic basal diameter ratio with a left apical 4-chamber view was 1.17. In addition, there was myocardial hypokinesis of the RV free wall using the B-mode. The interventricular septal flattening at end-systole and end-diastole (Fig. 2A), and paradoxical septal motion were observed with a right parasternal short axis view (Fig. 2B). Although mild tricuspid regurgitation (TR) with a normal valve morphology was observed on color Doppler, the velocity of TR was high (maximum velocity, 4.6 m/sec) (Fig. 2C), and the RA pressure was estimated as 10 mmHg because RA dilation was present without right-sided congestive heart failure [8]. The systolic PA pressure was estimated by calculating the peak TR gradient using the simplified Bernoulli equation: systolic PA pressure=4 ×(peak TR velocity)^2 + RA pressure. The estimated systolic PA pressure was 93.4 mmHg. These findings were consistent with severe PH. A thrombus was not detected in the RV, RA or PA on echocardiography. The pulsed-wave Doppler flow profile of PA was asymmetrical with mid-systolic notching (Fig. 2D). The PA acceleration time was 35 msec, the PA ejection time was 204 msec, and the acceleration time/ejection time ratio was 0.17. Mitral regurgitation was not identified. The transmitral flow pattern was an impaired relaxation pattern (E velocity, 0.55 m/sec; A velocity, 0.69 m/sec; E/A, 0.80).

Echocardiographic indices of the RV function, including peak systolic tricuspid annular velocity, tricuspid annulus plane systolic excursion, fractional area change, Tei index, RV free wall and septal longitudinal strain, and standard deviation of the time to peak longitudinal strain of the RV (RV-SD), which is the index of RV dyssynchrony, were also assessed [12]. Peak systolic tricuspid annular velocity was measured using tissue Doppler at the lateral tricuspid annulus with an apical 4-chamber view. Tricuspid annulus plane systolic excursion was measured using M-mode at the lateral tricuspid annulus with an apical 4-chamber view. Fractional area change was calculated as (RV end-diastolic area -RV end-systolic area)/RV end-diastolic area ×100. Right ventricular end-diastolic and end-systolic area were obtained by tracing the RV endocardium with the modified apical 4-chamber view for the right heart. Tei index was calculated as the sum of the isovolumic contraction time and isovolumic relaxation time divided by ejection time using tissue Doppler at the lateral tricuspid annulus with an apical 4-chamber view. RV free wall and septal longitudinal strain and RV-SD were measured by speckle tracking echocardiography using conventional gray-scale echocardiography with modified apical 4-chamber view. Speckle tracking echocardiography was performed using a previously described method with offline software (2D Wall Motion Tracking, Canon Medical Systems Corporation, Utsunomiya, Tochigi, Japan) [12]. Echocardiographic indices of the RV function were impaired in the present case compared with the reference interval of healthy dogs (Table 1) [12]. In addition, RV-SD was significantly increased in the present case (Table 1). This finding suggests that RV dysfunction and dyssynchrony occurred in this dog.

Based on radiography and echocardiography, several heart diseases causing PH, such as left-sided heart disease and congenital cardiac shunts were excluded. In this case, a tentative diagnosis was PH due to lung disease or PTE. To clarify the cause of PH,

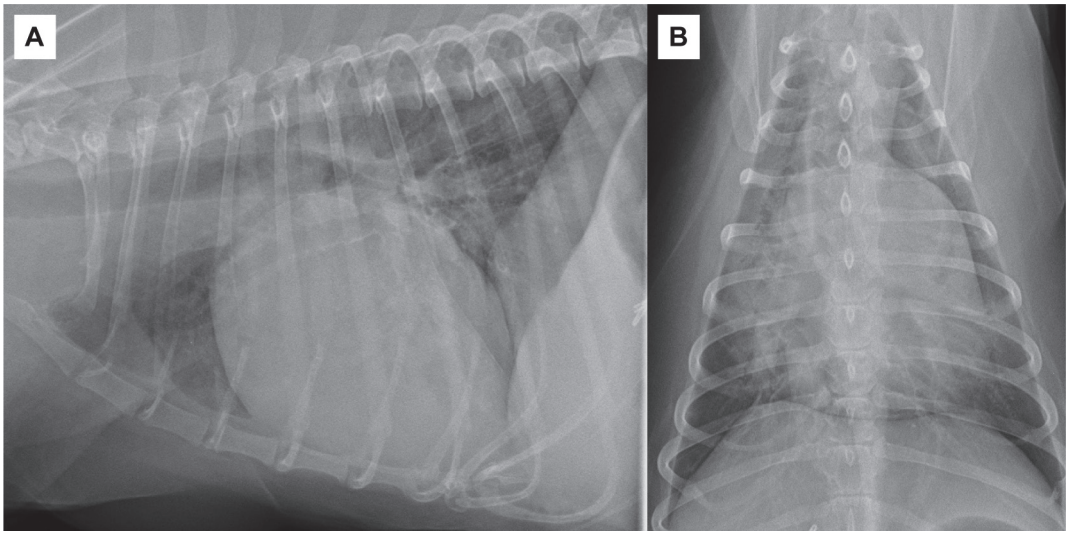

Fig. 1. Thoracic radiography on day 1. A) Right lateral thoracic radiograph showing cardiac enlargement (VHS 11.75). B) Dorsoventral thoracic radiograph showing enlargement of the main pulmonary artery in the left and right caudal lobes, and interstitial and alveolar lung patterns in the right cranial, middle, and left cranial lobes.

Table 1. Echocardiographic variables in present case on days 1 and 9

Variables	Day 1	Day 9	Reference interval [13, 14]
LVIDd (mm)	22.6	25.2	
RVIDd (mm)	15.1	8.4	
RV/LV	1.17	0.67	
RVWTd (mm)	3.4	4.4	
PA/Ao	1.24	1.15	0.93 ± 0.09
Transmitral E velocity (m/sec)	0.55	0.57	
Transmitral A velocity (m/sec)	0.69	0.9	
Transmitral E/A	0.8	0.6	
TR velocity (m/sec)	4.6	2.9	<3.0
Estimated systolic PAP (mmHg)	93.4	38.2	<41.0
AT (msec)	35	46	93 ± 16
ET (msec)	204	219	
AT/ET	0.17	0.21	0.46 ± 0.06
S'_{TV} (cm/sec)	10.5	16.2	12.8 ± 3.4
TAPSE (mm)	7.9	11.4	13.0 ± 2.4
FAC (%)	24.7	42.8	38.3 ± 6.8
Tei index by TDI	0.62	0.47	0.53 ± 0.05
Free wall longitudinal strain (%)	–7.3	–18.4	–19.0 ± 2.6
Septal longitudinal strain (%)	–6.0	–13.4	–15.7 ± 2.0
RV-SD6 (msec)	83.4	18.3	12.9 ± 6.7

AT, acceleration time; ET ejection time; LVIDd, left ventricular internal diameter in diastole; PA/Ao, pulmonary artery to aorta diameter ratio; PAP, pulmonary arterial pressure; RVIDd, right ventricular internal diameter in diastole; RV/LV, right ventricular to left ventricular end-diastolic basal diameter ratio; RV-SD6, standard deviation of the time to peak longitudinal strain of the right ventricle; RVWTd, right ventricular wall thickness in diastole; S'_{TV}, peak systolic tricuspid annular velocity; TAPSE, tricuspid annular plane systolic excursion; FAC, fractional area change; TDI, tissue Doppler; TR, tricuspid regurgitation.

CT angiography was acquired without general anesthesia with a 16-slice helical CT scanner (Activion16, Toshiba Medical Science Corp., Utsunomiya, Japan). CT angiography demonstrated the filling defect in left and right main PA (Fig. 3A and 3B). In addition, the filling defect in left and right brachiocephalic veins and right external jugular vein also were observed (Fig. 3C). Atelectasis in the middle lobe (Fig. 3D), and PA and RV dilation were observed. In addition, there were focal peribronchovascular consolidations with ground-grass opacity in the right cranial and left cranial and caudal lung lobes (Fig. 3D).

Based on these findings, the present case was diagnosed as acute PTE with severe PH. The dog was treated in the intensive care unit, and oxygen therapy (FiO2 0.40) was initiated. Low molecular heparin (200 IU/kg/day CRI, Fragmin, Kissei Pharmaceutical Corp., Tokyo, Japan) and cefazolin sodium hydrate (20 mg/kg IV *q* 12 hr, Cefamezin α, Astellas Pharma Inc., Tokyo, Japan) were administered. The combination of aspirin (0.5 mg/kg PO *q* 12 hr, Aspirin, Phizer Japan Inc., Tokyo, Japan) and clopidogrel sulfate (1.25 mg/kg PO *q* 12 hr, Plavix, Sanofi K.K., Tokyo, Japan) was administered in expectation of more effective anti-platelet effect. The respiratory status gradually improved during hospitalization. On day 9 of hospitalization, the dog showed a good clinical condition, breathing normally in room air. Echocardiographic variables on day 9 are summarized in Table 1. Echocardiography revealed a reduction in the size of the right heart, improvement in interventricular septal flattening, and decrease in the velocity of TR (maximum velocity, 2.9 m/sec; pressure gradient, 33 mmHg) (Fig. 4A and 4B). In addition, the hypokinesis of the RV free wall was improved, and RV dyssynchrony was also improved. CT angiography demonstrated that filling defects in the left and right pulmonary arteries and brachiocephalic veins had not changed (Fig. 5A–C). In contrast, the abnormal findings in lung field (focal peribronchovascular consolidations with ground-grass opacity) disappeared (Fig. 5D). The dog was discharged from hospital on day 10.

The plasma D-dimer (7.19 μg/m*l* [reference range, <1.0 μg/m*l*]) and fibrin degradation product (24.0 μg/m*l* [reference range, <5.0 μg/m*l*]) concentrations were elevated on day 1.

The present case was diagnosed as acute PTE by CT angiography. Several diseases and conditions, such as immune-mediated hemolytic anemia, hyperadrenocorticism, neoplasia, protein-losing nephropathy, sepsis, trauma, and surgery, have been associated with PTE in dogs [4]. In the present case, acute PTE occurred after surgery and prolonged cage rest. In human medicine, the most common cause of PTE is deep vein thrombosis, frequently in the lower extremities [9]. To our best knowledge, there are no report of the venous thrombosis of the lower extremities (hind limb) in dogs. In the present case, the thrombosis of brachiocephalic veins and external jugular vein were observed by CT angiography. Since the posture and blood vessel course is different between humans and dogs, the common site of venous thrombosis may be different between animal species. Therefore, extensive CT angiography including neck region may be recommended in dogs with suspected PTE.

The definitive diagnosis of PTE is made by CT angiography. A previous human study showed the high sensitivity and specificity of CT angiography to diagnose patients with acute PTE (sensitivity of 83% and specificity of 96%) [15]. However, CT angiography

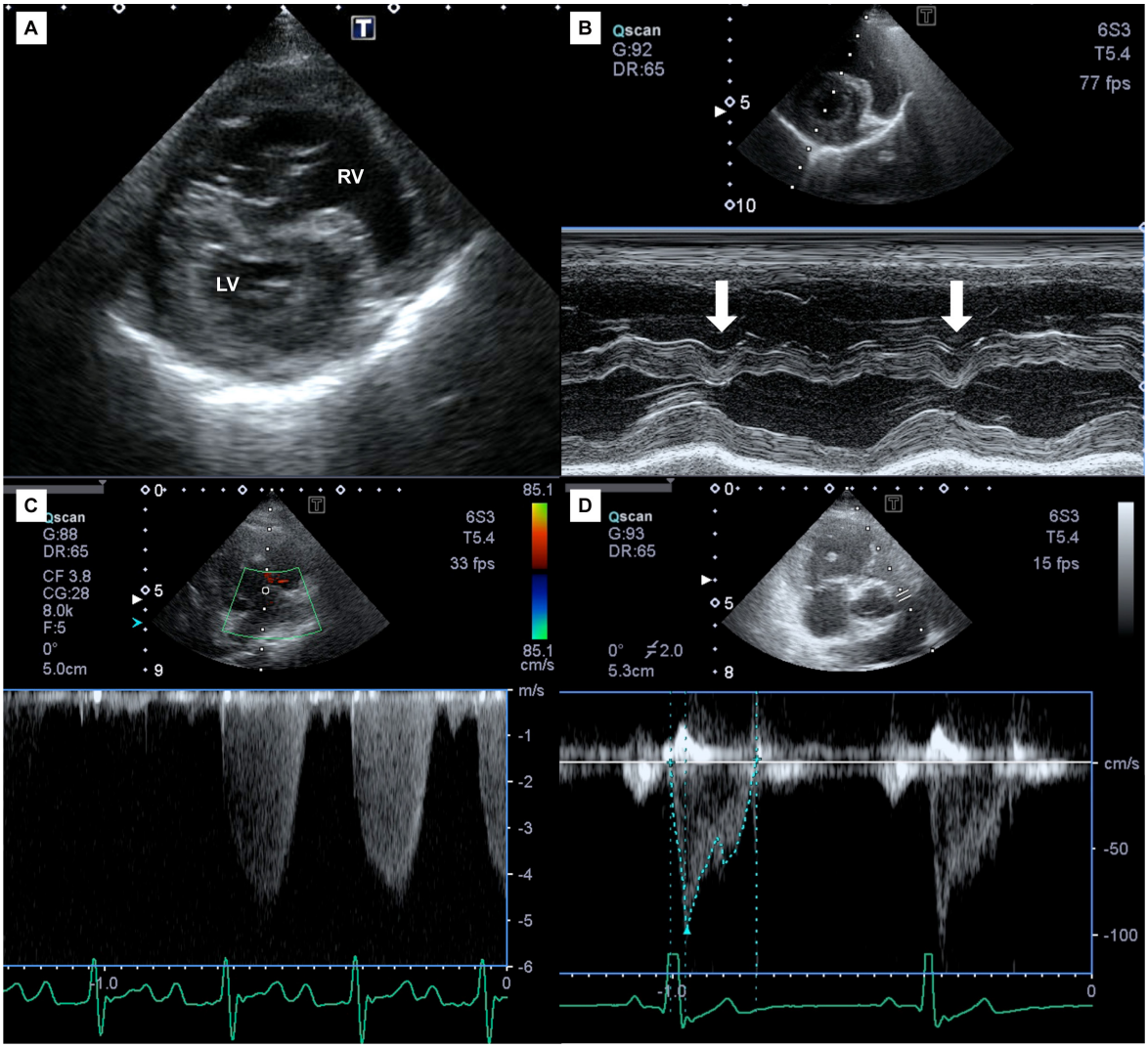

Fig. 2. Transthoracic echocardiography on day 1. A) Transthoracic echocardiography recorded with a right parasternal short axis view at the level of the papillary muscle. The right ventricle was severely dilated and interventricular septum was flattened at end-systole. B) M-mode image recorded with a right parasternal short axis view at the level of the papillary muscle showed paradoxical septal motion (white arrow). C) Continuous-wave Doppler image of tricuspid regurgitation. D) Pulsed-wave Doppler image of PA flow was asymmetrical with mid-systolic notching.

is not widely performed in dogs with suspected acute PTE.

Echocardiography is another diagnostic tool for PTE in human medicine. However, there are few reports on detailed echocardiographic findings in dogs with acute PTE. The human patients with acute PTE have RV dilation, septal flattening, PH, RV dysfunction and dyssynchrony [6, 16]. Only a previous retrospective study demonstrated that 5 of 29 dogs with acute PTE were examined by echocardiography, 2 of these dogs presented with RV and PA dilation, and only 1 dog had PH [7]. Similar to human patients, the present case had RV and PA dilation, septal flattening, RV free wall hypokinesis, PH, impaired echocardiographic indices of RV function, and RV dyssynchrony. However, these echocardiographic findings have a low specificity for acute PTE, and they can be detected in the setting of acute PH [2, 5, 11]. Our previous study using dog models of acute RV pressure overload also demonstrated that acute RV pressure overload caused RV dysfunction and dyssynchrony [13].

More specific echocardiographic signs of acute PTE, such as the McConnell sign, defined as hypokinesis of the RV free wall with normal contraction of the apical segment; 60/60 sign, the coexistence of shortened PA ejection time (<60 msec) with mid-systolic notching and TR pressure gradient <60 mmHg; and right heart thrombus, were reported as potentially useful "rule-in tests" due to high specificity and low sensitivity in human patients with acute-onset dyspnea [3, 10]. However, the present dog did not have these 3 specific echocardiographic findings. Further study is needed to validate whether these 3 specific echocardiographic findings are useful for diagnosing dogs with acute PTE.

In the present case, the impaired echocardiographic findings were improved with the relief of clinical symptoms by the treatment despite lack of improvement in filling defect in the PA assessed by CT angiography. Therefore, echocardiography can

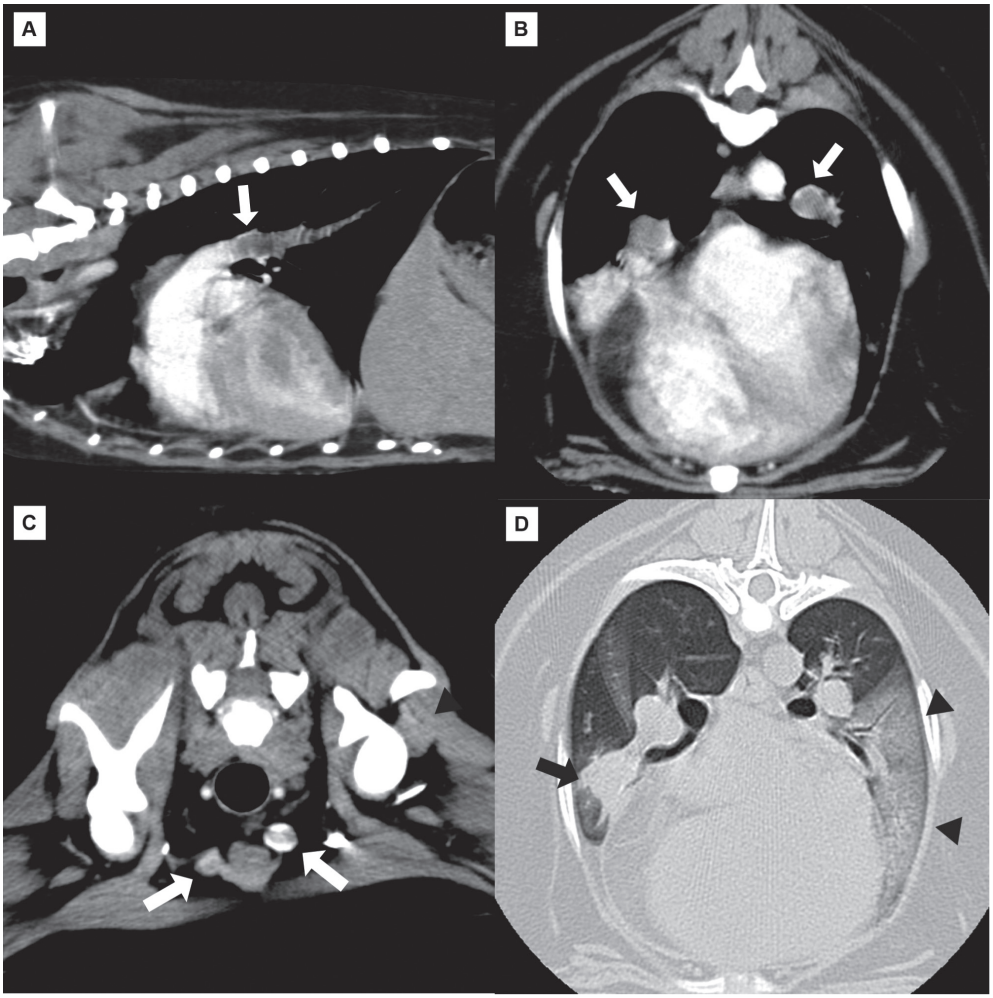

Fig. 3. CT image on day 1. A) Sagittal CT image showing the filling defect in left main pulmonary artery (white arrow). B) Axial CT imaging showing the filling defect in left and right main pulmonary arteries (white arrows). C) Axial CT imaging showing the filling defect in left and right brachiocephalic veins (white arrows). D) Axial CT imaging showing atelectasis in the middle lobe (black arrow), and ground-grass opacity in the caudal part of the left cranial lobe (black arrowheads).

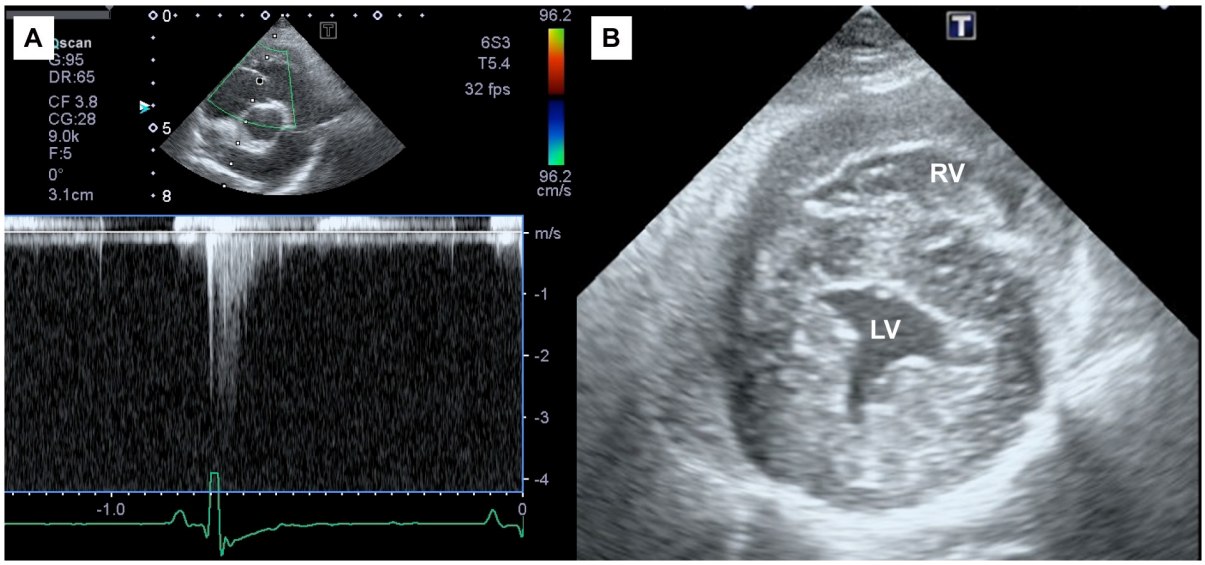

Fig. 4. Transthoracic echocardiography on day 9. A) Continuous-wave Doppler image of tricuspid regurgitation. The velocity of tricuspid regurgitation decreased compared to day 1. B) The right ventricle was not dilated and the interventricular septum was not flattened.

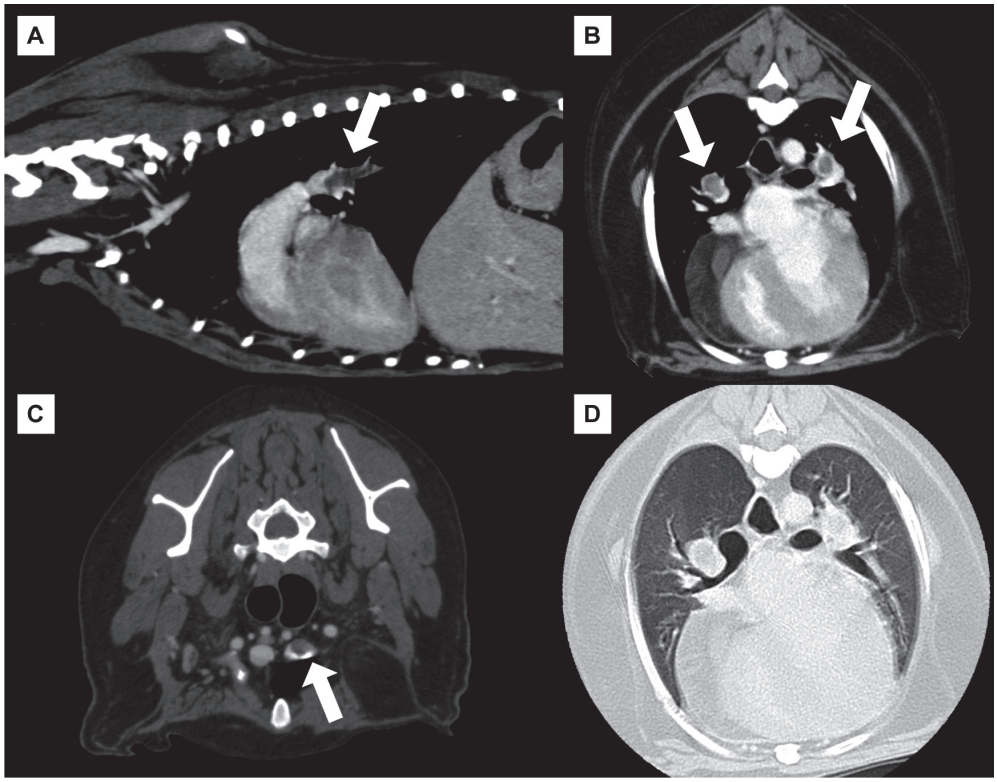

Fig. 5. CT image on day 9. A) Sagittal CT image showing the filling defect in left main pulmonary artery (white arrow). B) Axial CT imaging showing the filling defect in left and right main pulmonary arteries (white arrows). C) Axial CT imaging showing the filling defect in left and right brachiocephalic veins (white arrow). D) Axial CT imaging. There was no abnormality in lung field.

be useful for monitor of therapeutic efficacy in dogs with PTE. The reason for amelioration of clinical sign and improvement in echocardiographic findings may be attenuation of PH due to prevention of further thrombus formation and development of collateral circulation. Another reason may be improvement in ventilation-perfusion mismatch and hypoxia caused by PTE. While the abnormality in lung field assessed by CT angiography was disappeared, arterial blood gas analysis and ventilation-perfusion scan were not performed in the present case. Therefore, it is unknown whether ventilation-perfusion mismatch and hypoxia were improved or not.

In conclusion, this report describes the echocardiographic findings of acute PTE diagnosed by CT in a dog. These echocardiographic findings were reversed after anticoagulant therapy and oxygen supplementation. The findings reported here may be useful for the diagnosis and the monitor of therapeutic efficacy of dogs with acute PTE when CT is not feasible in a clinical setting.

REFERENCES

1. Bodey, A. R. and Michell, A. R. 1996. Epidemiological study of blood pressure in domestic dogs. *J. Small Anim. Pract.* **37**: 116–125. [Medline] [CrossRef]
2. Bova, C., Greco, F., Misuraca, G., Serafini, O., Crocco, F., Greco, A. and Noto, A. 2003. Diagnostic utility of echocardiography in patients with suspected pulmonary embolism. *Am. J. Emerg. Med.* **21**: 180–183. [Medline] [CrossRef]
3. Fields, J. M., Davis, J., Girson, L., Au, A., Potts, J., Morgan, C. J., Vetter, I. and Riesenberg, L. A. 2017. Transthoracic echocardiography for diagnosing pulmonary embolism: a systematic review and meta-analysis. *J. Am. Soc. Echocardiogr.* **30**: 714–723.e4. [Medline] [CrossRef]
4. Goggs, R., Benigni, L., Fuentes, V. L. and Chan, D. L. 2009. Pulmonary thromboembolism. *J. Vet. Emerg. Crit. Care (San Antonio)* **19**: 30–52. [Medline] [CrossRef]
5. Grifoni, S., Olivotto, I., Cecchini, P., Pieralli, F., Camaiti, A., Santoro, G., Pieri, A., Toccafondi, S., Magazzini, S., Berni, G. and Agnelli, G. 1998. Utility of an integrated clinical, echocardiographic, and venous ultrasonographic approach for triage of patients with suspected pulmonary embolism. *Am. J. Cardiol.* **82**: 1230–1235. [Medline] [CrossRef]
6. Hsiao, S. H., Lee, C. Y., Chang, S. M., Yang, S. H., Lin, S. K. and Huang, W. C. 2006. Pulmonary embolism and right heart function: insights from myocardial Doppler tissue imaging. *J. Am. Soc. Echocardiogr.* **19**: 822–828. [Medline] [CrossRef]
7. Johnson, L. R., Lappin, M. R. and Baker, D. C. 1999. Pulmonary thromboembolism in 29 dogs: 1985–1995. *J. Vet. Intern. Med.* **13**: 338–345. [Medline]
8. Kittleson, M. and Kienle, R. 1998. Pulmonary arterial and systemic arterial hypertension. pp. 433–449. *In*: Small Animal Cardiovasular Medicine (Kittleson M, Kienle R eds), Mosby, St. Louis.
9. Konstantinides, S. V., Torbicki, A., Agnelli, G., Danchin, N., Fitzmaurice, D., Galiè, N., Gibbs, J. S. R., Huisman, M. V., Humbert, M., Kucher,

N., Lang, I., Lankeit, M., Lekakis, J., Maack, C., Mayer, E., Meneveau, N., Perrier, A., Pruszczyk, P., Rasmussen, L. H., Schindler, T. H., Svitil, P., Vonk Noordegraaf, A., Zamorano, J. L., Zompatori M., Task Force for the Diagnosis and Management of Acute Pulmonary Embolism of the European Society of Cardiology (ESC). 2014. 2014 ESC guidelines on the diagnosis and management of acute pulmonary embolism. *Eur. Heart J.* **35**: 3033–3069, 3069a–3069k. [Medline] [CrossRef]
10. Kurnicka, K., Lichodziejewska, B., Goliszek, S., Dzikowska-Diduch, O., Zdończyk, O., Kozłowska, M., Kostrubiec, M., Ciurzyński, M., Palczewski, P., Grudzka, K., Krupa, M., Koć, M. and Pruszczyk, P. 2016. Echocardiographic pattern of acute pulmonary embolism: analysis of 511 consecutive patients. *J. Am. Soc. Echocardiogr.* **29**: 907–913. [Medline] [CrossRef]
11. Miniati, M., Monti, S., Pratali, L., Di Ricco, G., Marini, C., Formichi, B., Prediletto, R., Michelassi, C., Di Lorenzo, M., Tonelli, L. and Pistolesi, M. 2001. Value of transthoracic echocardiography in the diagnosis of pulmonary embolism: results of a prospective study in unselected patients. *Am. J. Med.* **110**: 528–535. [Medline] [CrossRef]
12. Morita, T., Nakamura, K., Osuga, T., Yokoyama, N., Khoirun, N., Morishita, K., Sasaki, N., Ohta, H. and Takiguchi, M. 2017. The repeatability and characteristics of right ventricular longitudinal strain imaging by speckle-tracking echocardiography in healthy dogs. *J. Vet. Cardiol.* **19**: 351–362. [Medline] [CrossRef]
13. Morita, T., Nakamura, K., Osuga, T., Yokoyama, N., Morishita, K., Sasaki, N., Ohta, H. and Takiguchi, M. 2017. Changes in right ventricular function assessed by echocardiography in dog models of mild RV pressure overload. *Echocardiography* **34**: 1040–1049. [Medline] [CrossRef]
14. Serres, F., Chetboul, V., Gouni, V., Tissier, R., Sampedrano, C. C. and Pouchelon, J. L. 2007. Diagnostic value of echo-Doppler and tissue Doppler imaging in dogs with pulmonary arterial hypertension. *J. Vet. Intern. Med.* **21**: 1280–1289. [Medline] [CrossRef]
15. Stein, P. D., Fowler, S. E., Goodman, L. R., Gottschalk, A., Hales, C. A., Hull, R. D., Leeper, K. V. J. Jr., Popovich, J. Jr., Quinn, D. A., Sos, T. A., Sostman, H. D., Tapson, V. F., Wakefield, T. W., Weg, J. G., Woodard P. K., PIOPED II Investigators. 2006. Multidetector computed tomography for acute pulmonary embolism. *N. Engl. J. Med.* **354**: 2317–2327. [Medline] [CrossRef]
16. Sugiura, E., Dohi, K., Onishi, K., Takamura, T., Tsuji, A., Ota, S., Yamada, N., Nakamura, M., Nobori, T. and Ito, M. 2009. Reversible right ventricular regional non-uniformity quantified by speckle-tracking strain imaging in patients with acute pulmonary thromboembolism. *J. Am. Soc. Echocardiogr.* **22**: 1353–1359. [Medline] [CrossRef]